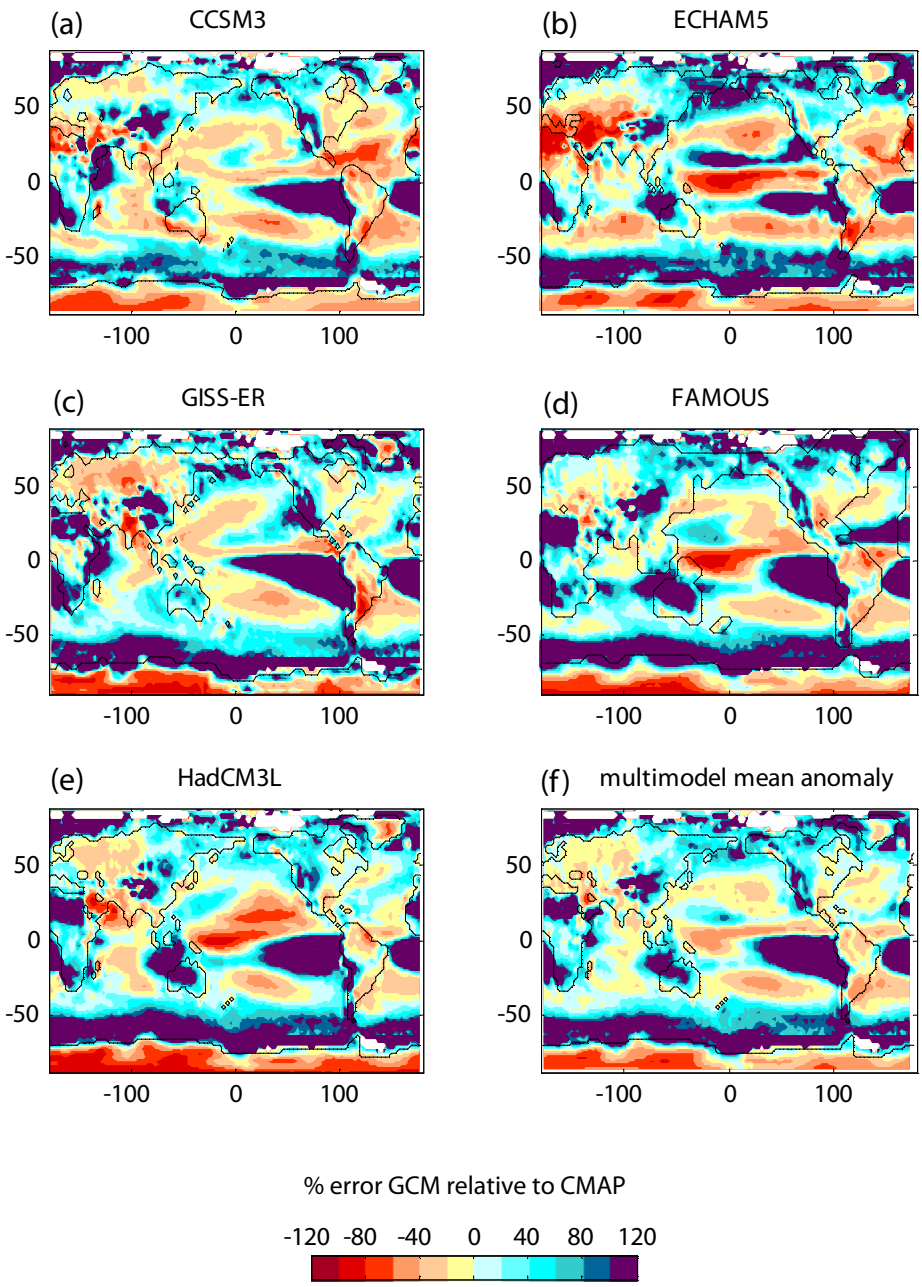

Figure S1 Percentage error between preindustrial model simulated mean annual precipitation and CMAP observational data, calculated as (model-observations)/observations x 100%

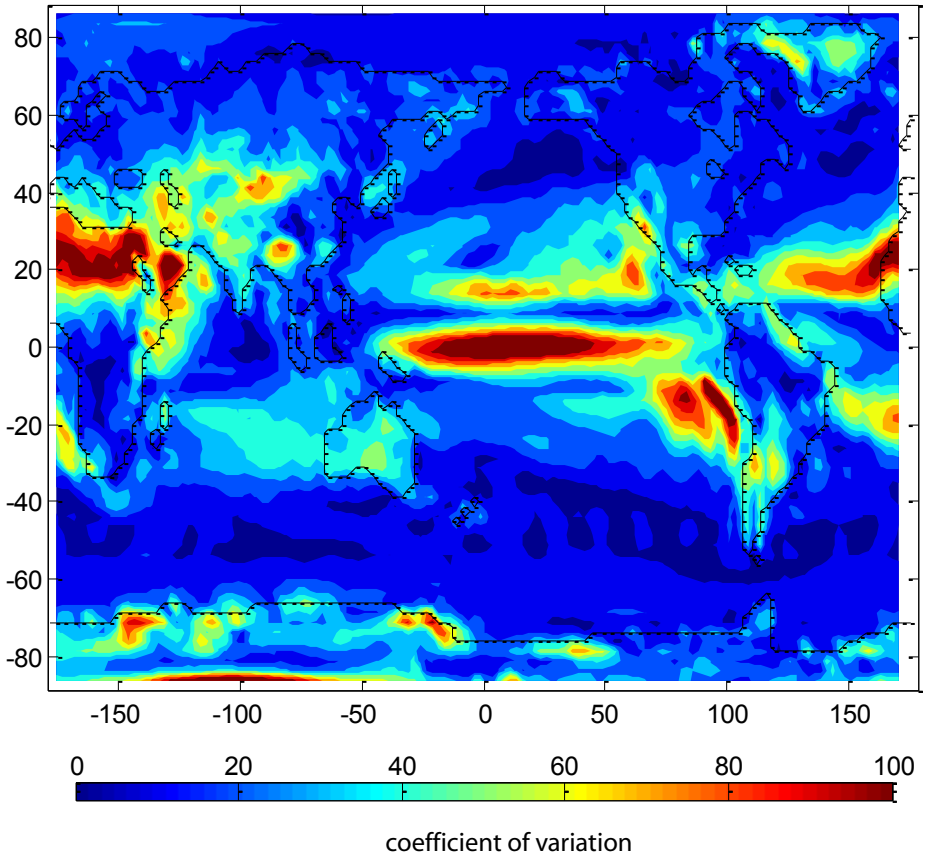

Figure S2 Coefficient of variation for preindustrial model simulations, calculated as standard deviation of multi-model mean (n=5) divided by multi-model mean. This is robust against larger standard deviations in regions of higher precipitation.

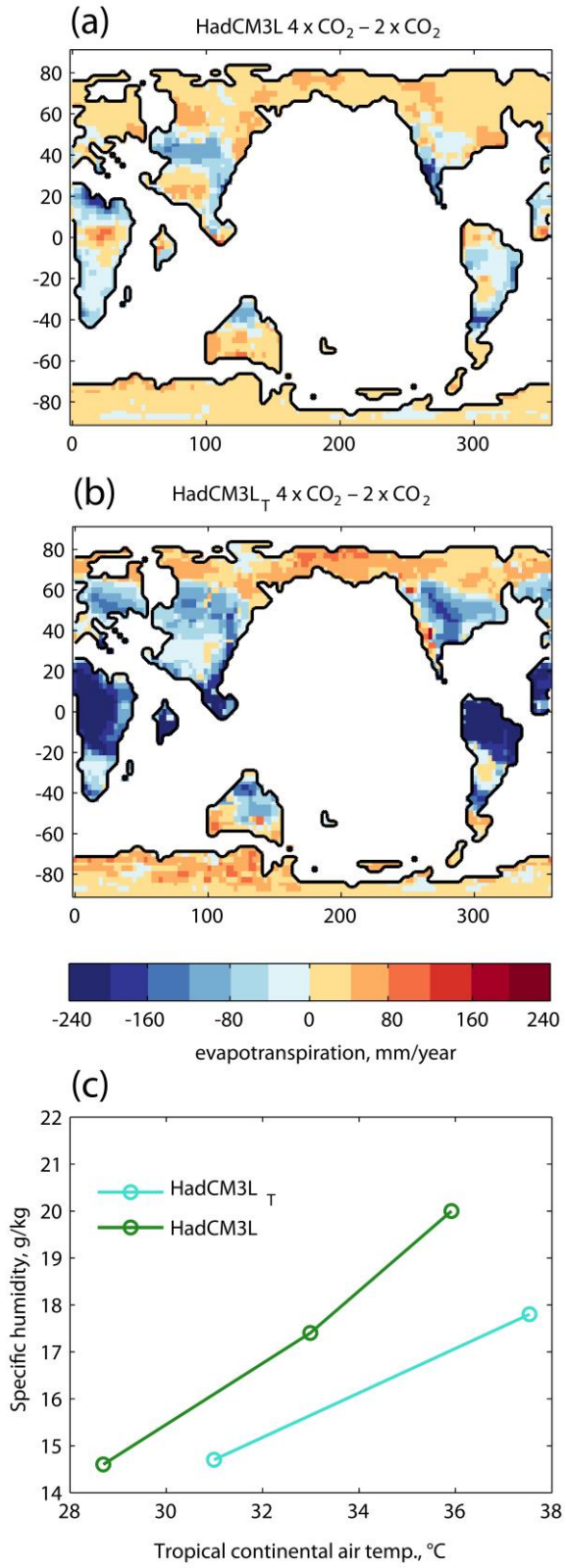

Figure S3 Changes in mean annual evapotranspiration 4 x CO_2 – 2 CO_2 in HadCM3L simulations in **(a)** the fixed shrubland simulations of Lunt et al. (2010) and **(b)** the TRIFFID dynamic vegetation simulations of Loptson et al. (2014). The differences in mean specific humidity relative to air temperature over tropical continents is shown in **(c)**.

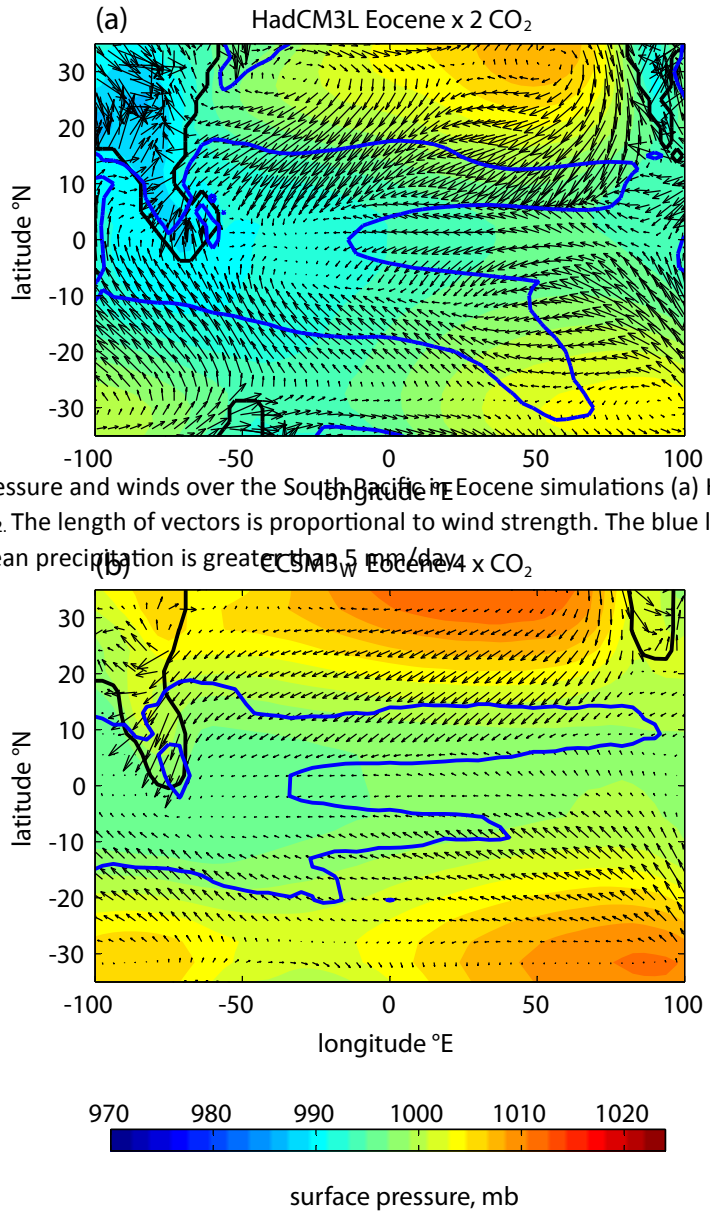

Figure S4 Surface pressure and winds over the South Pacific in Eocene simulations (a) HadCM3L, 2 x CO_2 and (b) CCSM3W, 4 x CO_2. The length of vectors is proportional to wind strength. The blue line shows the outline of the region where mean precipitation is greater than 5 mm/day.

Figure S4 Surface pressure and winds over the South Pacific in Eocene simulations **(a)** HadCM3L, 2 x CO2 and **(b)** CCSM3W, 4 x CO2. The length of vectors is proportional to wind strength. The blue line shows the outline of the region where mean precipitation is greater than 1800 mm/year (5 mm/day).

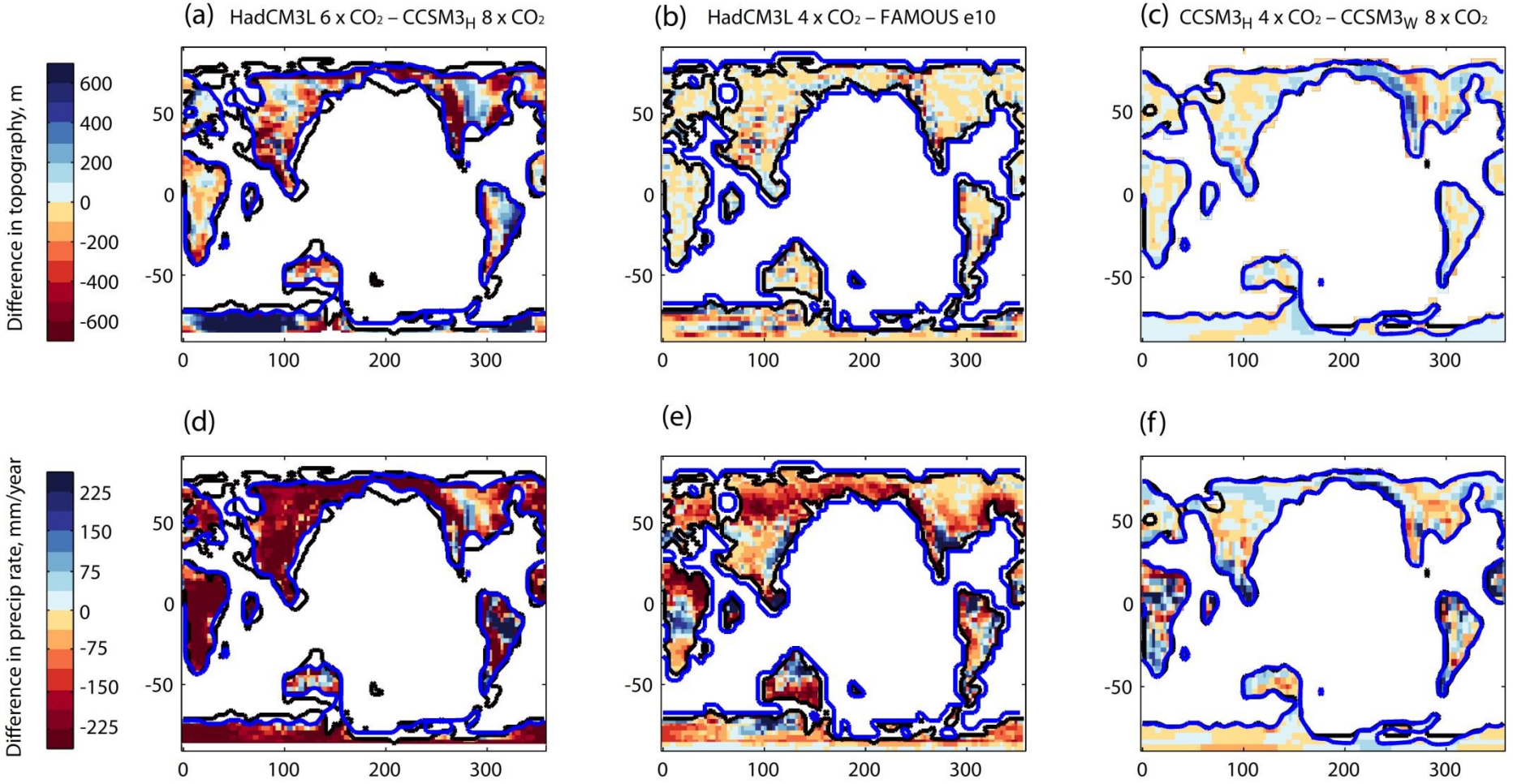

Figure S5 Differences in topography **(a – c)** and precipitation rate **(d – f)** in pairs of simulations; HadCM3L 6 x CO_2 – CCSM3(H) 8 x CO_2 **(a,d)**; HadCM3L 4 x CO_2 – FAMOUS e10 **(b,e)** and CCSM3(H) 4 x CO_2 and CCSM3(W) 8 x CO_2 **(c,f)**. Simulations are chosen which have similar global precipitation rates (Figure 2).

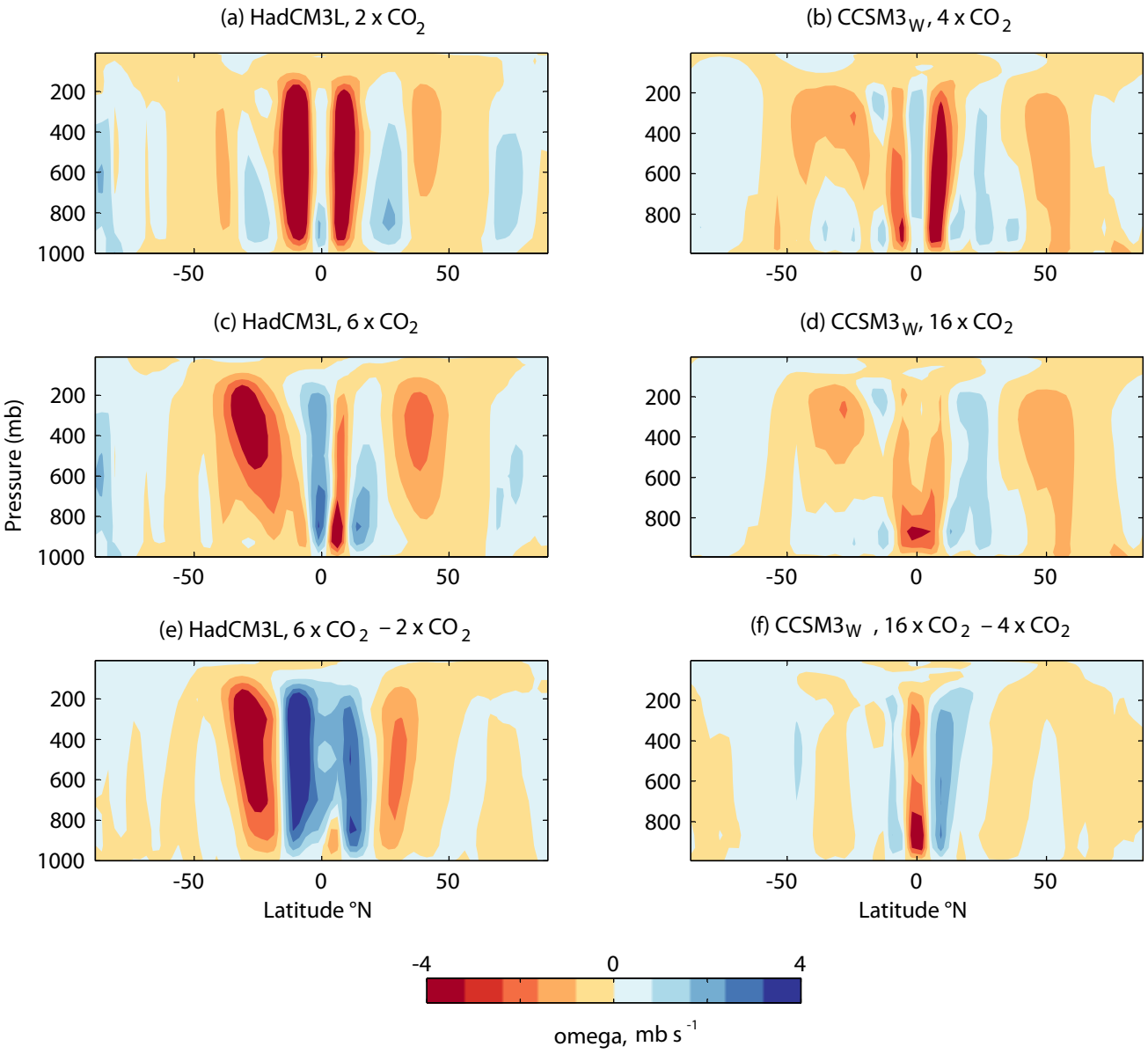

Figure S6 Vertical velocity of atmosphere averaged over 150°E to 150°W for HadCM3L simulations (**a, c**) and CCSM3(W) simulations (**b, d**). Anomalies for the high CO_2 – low CO_2 simulations are shown in (**e**) and (**f**).

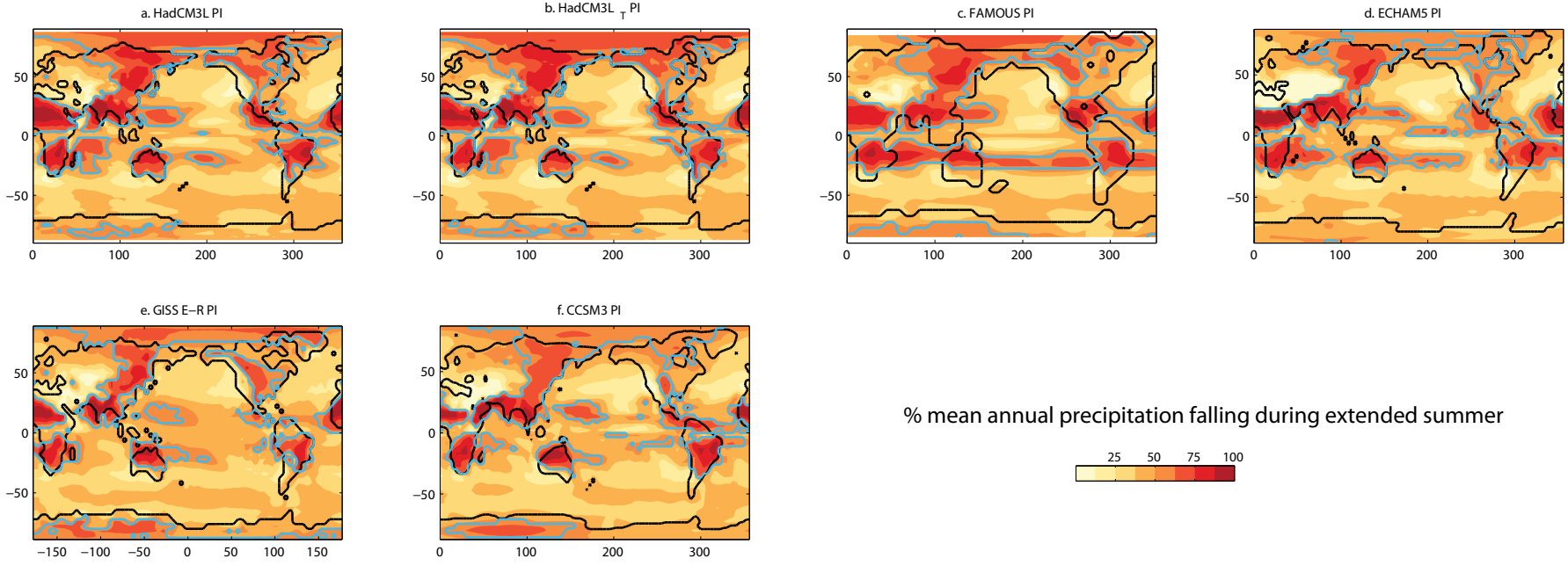

Figure S7 Percentage of mean annual precipitation falling in the extended summer season (MJJAS for northern hemisphere, NDJFM for southern hemisphere) for preindustrial simulations; regions with >55% summer precipitation are outlined in blue.

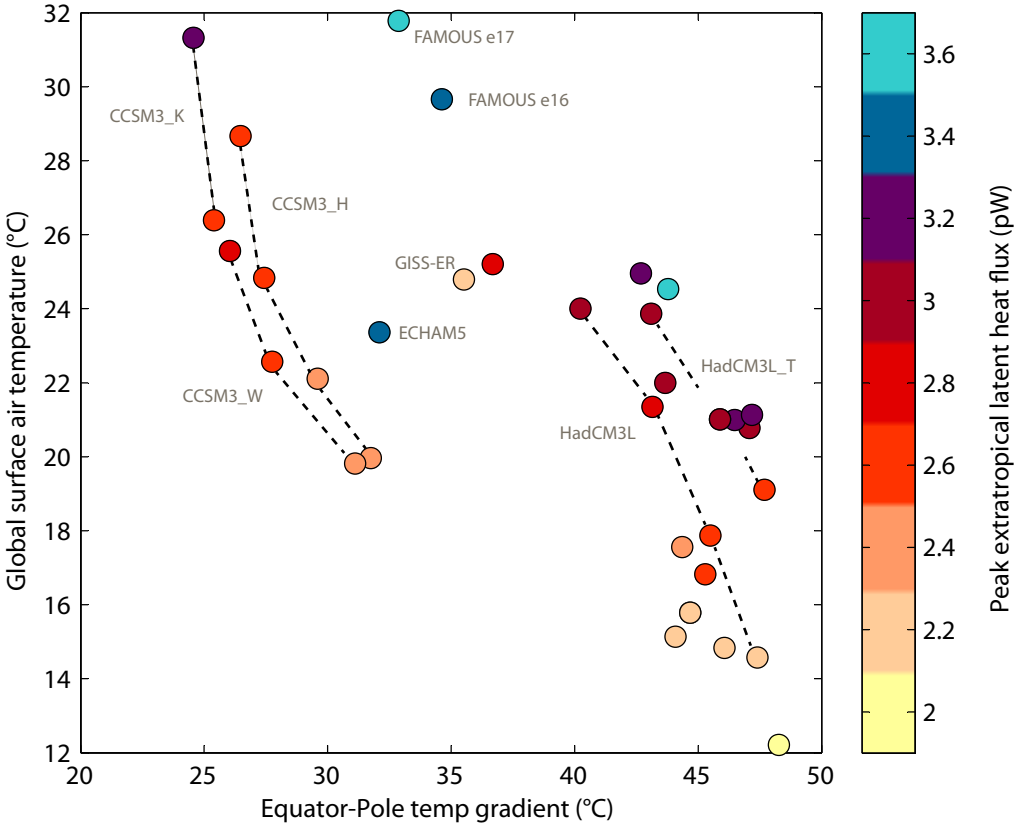

Figure S8 Variations in the peak extratropical (>25°N/S) latent heat flux in petawatts (1 PW = 10^{15} W) between the EoMIP model simulations relative to global mean surface air temperature and the average difference in surface air temperature between the poles and equator. With the exception of the FAMOUS simulations of Sagoo et al. (2013), simulations performed with the same GCM are joined by dotted lines for clarity.

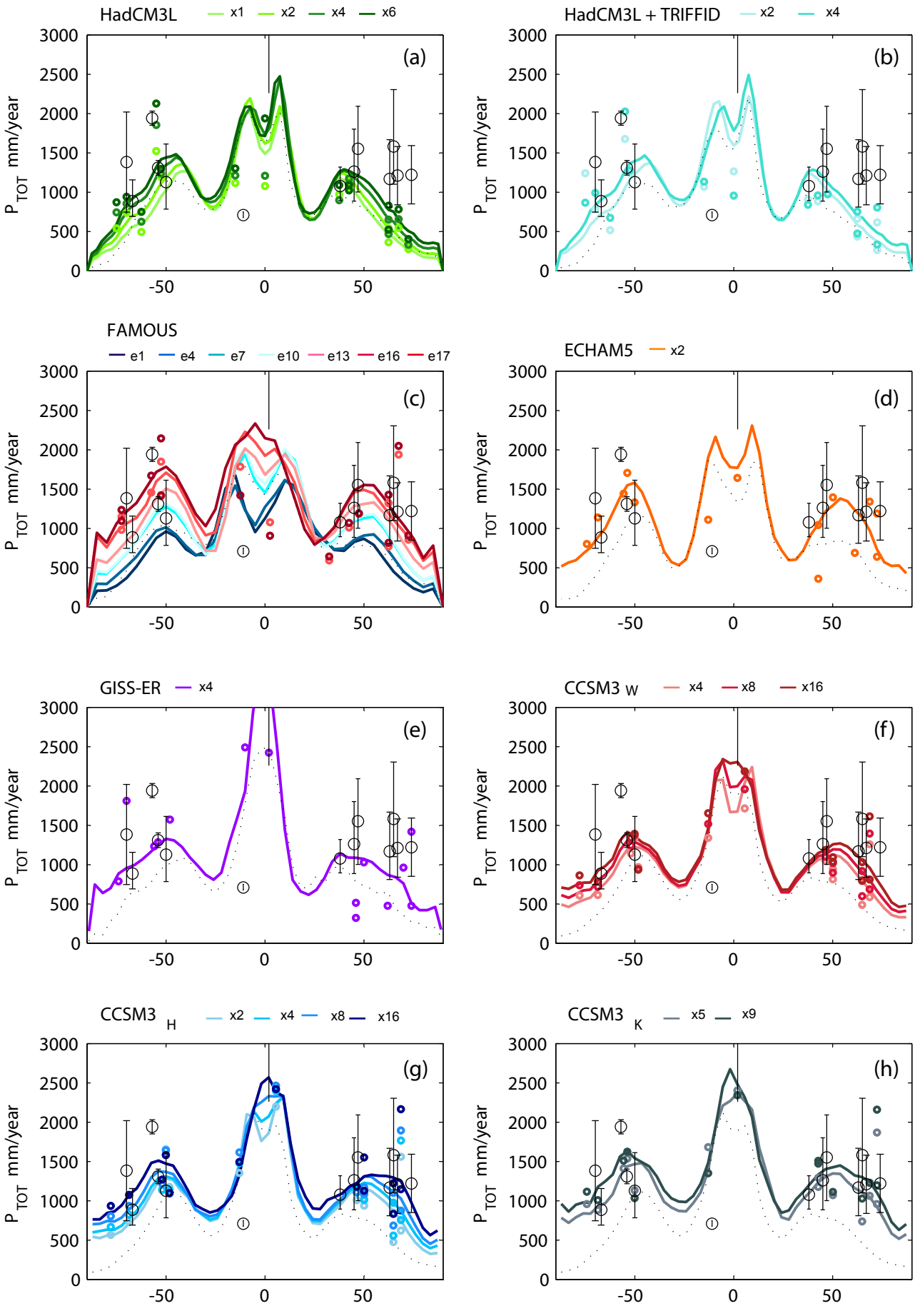

Figure S9 Proxy estimates of mean annual precipitation shown relative to latitudinal precipitation distribution (mm/year) for each of the EoMIP simulations. Model CO_2 or simulation name in the case of FAMOUS are shown above each panel. Preindustrial precipitation is shown as a black dotted line. Geologic data are represented by a lower, central and upper estimate based on combined data for the following sites: Wilkes Land, Antarctic Peninsula, southern Australia, New Zealand, Chile, Tanzania, Colombia, eastern China, continental US, central Europe, North West Territories, Alaska, Site 913 and Axel Heiberg Island. Model estimates from gridboxes corresponding to the paleo-locations are shown as coloured circles.

Simulation	Global mean precipitation (mm day^{-1})	Global mean evaporation (mm day^{-1})	Residual water mass (x 10^{12} kg day^{-1})	Latent heat forcing (x 10^{13} W)
HadCM3L				
Preindustrial	2.915	2.910	2.565	6.710
Eocene x1	3.007	3.005	1.254	3.279
Eocene x2	3.202	3.199	1.380	3.610
Eocene x4	3.376	3.372	1.707	4.465
Eocene x6	3.510	3.507	1.878	4.916
Preindustrial TRIFFID	2.866	2.866	0.2212	0.5786
Eocene x2 TRIFFID	3.233	3.233	0.1615	0.4225
Eocene x4 TRIFFID	3.415	3.415	0.1819	0.4758
ECHAM5				
Preindustrial	2.749	2.759	-5.154	-13.48
Eocene x2	3.423	3.433	-5.264	-13.77
GISS-ER				
Preindustrial	2.968	2.966	0.5774	1.510
Eocene x4	3.675	3.673	1.077	2.816
FAMOUS				
Preindustrial	2.908	2.912	-2.361	-6.176
E16	3.936	9.939	-1.545	-4.042
E17	4.135	4.137	-1.245	-3.255
CCSM3				
Preindustrial	2.650	2.648	1.164	3.044
Eocene H x2	3.288	3.285	1.082	2.830
Eocene H x4	3.415	3.413	1.121	2.932
Eocene Hx8	3.572	3.570	1.208	3.159
Eocene Hx16	3.790	3.780	5.062	13.24
Eocene Wx4	3.168	3.166	1.080	2.824
Eocene Wx8	3.332	3.330	1.166	3.049
Eocene Wx16	3.499	3.496	1.248	3.263
Eocene Kx5	3.678	3.677	1.321	3.455
Eocene Kx9	3.969	3.966	1.640	4.290

Table S1 Assessment of the imbalance between global precipitation and evaporation rates in the EoMIP ensemble. The imbalance is additionally shown as a global residual water mass and equivalent latent heat forcing.

	Preindustrial						Eo x 1 CO2	Eocene x 2 CO2					Eocene x 4 CO2					Eo x ~5 CO2	Eo x 6 CO2	Eocene x 8 CO2		Eo x ~9 CO2	Eocene x 16 CO2	
	HadCM	HadCM TRIFFID	FAMOUS	CCSM *	ECHAM	GISS	HadCM	HadCM	HadCM	FAMOUS E17	ECHAM	CCSM H	HadCM	HadCM	CCSM H	CCSM W	GISS	CCSM K	HadCM	CCSM H	CCSM W	CCSM K	CCSM H	CCSM W
Global P_{TOT}	2.91	2.87	2.91	2.65	2.75	2.97	3.01	3.20	3.23	4.13	3.42	3.29	3.38	3.42	3.42	3.17	3.67	3.68	3.51	3.57	3.33	3.97	3.79	3.50
Global P_{CV}		2.16	2.37	1.99	1.80		2.38	2.56	2.60	3.75	2.37	2.65	2.73	2.80	2.78	2.57		3.12	2.89	2.96	2.76	3.39	3.19	2.93
Global P_{LS}		0.71	0.54	0.66	0.95		0.63	0.64	0.63	0.39	1.05	0.63	0.64	0.62	0.63	0.60		0.56	0.62	0.61	0.58	0.58	0.60	0.57
Global P_{CV}/P_{TOT}		0.75	0.81	0.75	0.65		0.79	0.80	0.80	0.91	0.69	0.81	0.81	0.82	0.81	0.81		0.85	0.82	0.83	0.83	0.85	0.84	0.84
Global Temp /°C	12.72	11.87	14.36	11.62	13.54	13.79	14.57	17.87	19.11	31.77	23.36	19.96	21.35	23.86	22.10	19.82	24.79	26.39	24.00	24.83	22.56	31.32	28.67	25.56
Land P_{TOT}	2.14	2.20	2.62	1.90	1.81	2.45	2.08	2.25	2.29	3.22	2.57	3.11	2.40	2.36	3.36	2.90	3.12	3.66	2.65	3.61	3.18	3.93	3.86	3.43
Land P_{CV}		1.66	2.17	1.40	1.05		1.59	1.71	1.77	2.63	1.37	2.37	1.84	1.80	2.61	2.26		2.98	2.07	2.85	2.52	3.23	3.10	2.76
Land P_{LS}		0.54	0.44	0.50	0.76		0.49	0.54	0.52	0.60	1.21	0.74	0.56	0.55	0.75	0.64		0.69	0.58	0.76	0.66	0.70	0.76	0.67
Land P_{CV}/P_{TOT}		0.75	0.83	0.74	0.58		0.76	0.76	0.77	0.82	0.53	0.76	0.77	0.76	0.78	0.78		0.81	0.78	0.79	0.79	0.82	0.80	0.80
Land Temp /°C	6.26	5.65	10.64	6.18	7.70	8.19	8.05	12.07	14.64	30.01	20.90	16.24	16.54	21.03	18.93	16.71	21.98	24.65	20.14	22.17	19.99	30.68	26.85	23.59
Ocean P_{TOT}	3.23	3.14	3.12	2.96	3.12	3.18	3.38	3.59	3.62	4.80	3.74	3.35	3.77	3.85	3.43	3.26	3.87	3.68	3.86	3.56	3.38	3.98	3.77	3.52
Ocean P_{CV}		2.36	2.52	2.23	2.10		2.70	2.90	2.94	4.58	2.75	2.75	3.09	3.21	2.85	2.68		3.17	3.23	2.99	2.83	3.44	3.22	2.99
Ocean P_{LS}		0.76	0.61	0.73	1.02		0.68	0.69	0.68	0.23	0.99	0.60	0.68	0.64	0.59	0.58		0.52	0.63	0.57	0.55	0.54	0.55	0.53
Ocean P_{CV}/P_{TOT}		0.75	0.81	0.75	0.67		0.80	0.81	0.81	0.95	0.74	0.82	0.82	0.83	0.83	0.82		0.86	0.84	0.84	0.84	0.86	0.85	0.85
Land/Ocean P_{TOT}	0.66	0.70	0.84	0.64	0.58	0.77	0.62	0.63	0.63	0.67	0.69	0.93	0.64	0.61	0.98	0.89	0.81	0.99	0.69	1.01	0.94	0.99	1.02	0.97
Ocean Temp /°C	15.35	14.41	17.14	13.88	15.88	16.12	17.23	20.23	20.92	33.08	24.29	21.21	23.30	25.02	23.17	20.86	25.91	26.96	25.58	25.72	23.43	30.68	26.85	23.59

Table S2 Sensitivity of the global Eocene hydrological cycle. Rates shown represent annual mean precipitation mm day^{-1} globally and separately over land and ocean. TOT = total precipitation rate; CV = convective precipitation; LS = large-scale precipitation. Note that CV and LS sum to give total precipitation rate, but land and ocean represent averages over those regions; * CCSM_W, CCSM_H and CCSM_K share a preindustrial simulation.